

Current-induced conformational switching in single-molecule junctions

Florian Elste · Guillaume Weick · Carsten Timm · Felix von Oppen

Received: 4 February 2008 / Accepted: 9 July 2008 / Published online: 6 August 2008
© Springer-Verlag 2008

Abstract Current-induced conformational switching in single-molecule junctions constitutes a fundamental process in molecular electronics. Motivated by recent experiments on azobenzene derivatives, we study this process for molecules which exhibit two (meta)stable conformations in the neutral state but only a single stable conformation in the ionic state. We derive and analyze appropriate Fokker–Planck equations obtained from a density-matrix formalism starting from a generic model and present comprehensive analytical and numerical results for the switching dynamics in general and the quantum yield in particular.

PACS 73.63.-b · 85.65.+h · 73.23.Hk · 82.30.Qt

1 Introduction

Over the past few years the emerging field of molecular electronics has fueled the interest in understanding the physics of single-molecule transistors. Not only are there promising technological applications, it has also been shown that the presence of specific internal molecular degrees of freedom such as vibrations, spins, and different chemical con-

formations leads to numerous novel quantum transport phenomena that go beyond the physics observed in other nano-sized objects such as quantum dots [1–14]. An essential requirement for electric circuits of nanoscale dimensions is a molecular device that can be switched between two distinct conductive states. Because of intrinsic bistabilities, many single-molecule junctions reveal switching behavior, e.g., involving cis and trans isomers of a molecule [15–25].

In this context, various types of switching mechanisms that stimulate changes of the chemical conformation have been discussed in the literature [15]. Consider a molecule that is either in the cis or in the trans configuration modeled by a double-well potential as shown in Fig. 1(a). The potential surface is characterized by an energy barrier W between the two minima and an attempt frequency ω_0 , which is determined by the curvature at the local minimum. This energy barrier can be overcome by (i) thermal activation. The rate for this process is given by

$$\Gamma_{\text{thermal}} \simeq \frac{\omega_0}{2\pi} \exp\left(-\frac{W}{k_B T}\right). \quad (1)$$

For thermal energies $k_B T$ larger than the vibrational energy $\hbar\omega_0$, thermal activation dominates over (ii) quantum tunneling, cf. Fig. 1(b). Switching due to quantum tunneling is also exponentially suppressed,¹

$$\Gamma_{\text{quantum}} \simeq \frac{\omega_0}{2\pi} \exp\left(-\frac{W}{\hbar\omega_0/2\pi}\right). \quad (2)$$

F. Elste · G. Weick (✉) · F. von Oppen
Institut für Theoretische Physik, Freie Universität Berlin,
Arnimallee 14, 14195 Berlin, Germany
e-mail: weick@physik.fu-berlin.de

C. Timm
Department of Physics and Astronomy, University of Kansas,
Lawrence, KS 66045, USA

C. Timm
Institute for Theoretical Physics, Technische Universität Dresden,
01062 Dresden, Germany

¹In the expression for the switching rate due to quantum tunneling, the frequency in the exponential is actually determined by the curvature of the potential surface at the local maximum. However, since it is usually of the same order of magnitude as the attempt frequency ω_0 , we do not distinguish between the two frequencies.

Both thermal and quantum tunneling do not require the molecule to be out of equilibrium and, in principle, occur even at zero bias voltage. In addition, conformational switching can also be induced by the applied current, which drives the molecule out of equilibrium. (iii) Such *current-induced* switching can be triggered by tunneling events into and out of the molecule which are accompanied by the emission of a single vibron, as illustrated in Fig. 1(c). Assuming that all relevant charge states exhibit the same conformational bistability and ohmic response,

$$\Gamma_{\text{cur-ind}}(V) \simeq \frac{\lambda G}{e} (|V| - \hbar\omega_0/e) \Theta(|V| - \hbar\omega_0/e), \quad (3)$$

i.e., the rate for such processes is proportional to the phase space volume of electrons energetically available in the reservoirs determined by the bias voltage V . Here G is the conductance and λ the effective electron-vibron coupling strength. Equation (3) can be derived treating the electron-vibron coupling perturbatively [22]. (iv) The switching may also require several subsequent inelastic tunneling events to overcome the energy barrier between the cis and trans state, cf. Fig. 1(d). If the critical oscillator state where the transition becomes possible is given by n , the switching rate acquires the form [22]

$$\Gamma_{\text{cur-ind},n}(I) \sim I^n. \quad (4)$$

In order to observe such a power-law dependence on the current I , the excitation of vibrons has to be induced by the current, whereas vibrational de-excitation has to be dominated by *dissipative* rather than *current-induced* processes. The discussed switching mechanisms (i)–(iv) have been found to play an important role in oligo-phenylenevinylene (OPV3) derivatives which have recently been investigated by Danilov et al. [15] in a molecular junction.

In the present paper we consider molecules which exhibit conformational bistability only in the neutral state, while the potential surface of the ionic state has a single minimum. Due to an avoided level crossing, this minimum is typically in between the two minima of the double well, cf. Fig. 1(e), e.g., as approximately realized in azobenzene [26]. Our main focus is on the regime of strongly asymmetric couplings to the leads, corresponding to the experimental setup of a scanning tunneling microscope (STM) conductance measurement. Here the molecule is strongly coupled to the substrate, while the coupling to the tip is much weaker. This asymmetry has important consequences for the conductance and for the dynamics of the passage of charge carriers. For thermal energies large compared to the level-broadening due to the coupling to the leads, the stationary current is $I \sim e \Gamma_{\text{tip}} \Gamma_{\text{sub}} / (\Gamma_{\text{tip}} + \Gamma_{\text{sub}})$, where Γ_{tip} and Γ_{sub} are the tunneling-induced level widths due to the coupling to the tip and to the substrate, respectively. Thus, the current passing through an asymmetric junction is, to a good approximation, governed by the smaller rate only. The molecule spends

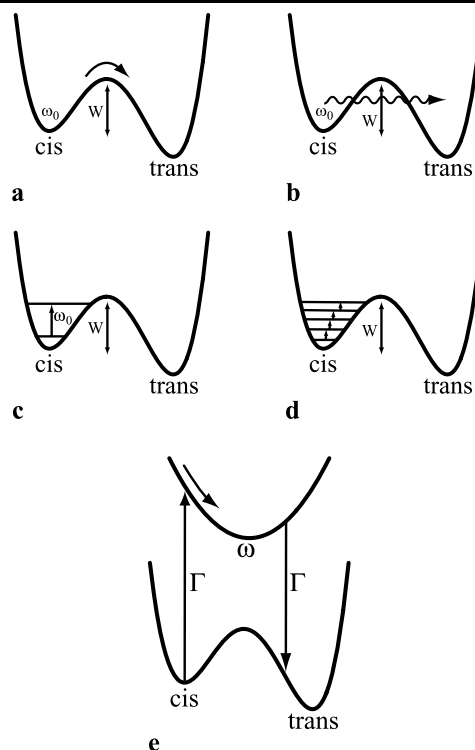


Fig. 1 Switching process induced by (a) thermal activation, (b) quantum tunneling, (c) vibrational-assisted tunneling involving the emission of a single phonon, and (d) the emission of several phonons. The switching process studied in the present paper is sketched in (e)

most of the time in the neutral state, i.e., whenever an electron tunnels from the tip onto the molecule, it continues into the substrate almost instantaneously, while the average waiting time until the next tunneling event from the tip is long.

The basic mechanism of current-induced switching now follows from the Franck–Condon principle, which states that the vibrational state does not change during the much faster electronic tunneling processes in and out of the molecule. The switching process is initiated by a first transition from one of the two conformational states into the charged state. After the molecule evolves on the potential surface of the charged state, it eventually undergoes a second tunneling transition from the charged state into a conformational state, cf. Fig. 1(e). Clearly, the switching probability strongly depends on the ratio of the vibrational frequency in the charged state, ω , and $\Gamma = \Gamma_{\text{tip}} + \Gamma_{\text{sub}}$. For $\omega \gg \Gamma$, the molecule oscillates many times between the two tunneling events, and the probabilities for transitions from the charged state into the two conformational states of the neutral molecule are of the same order. In contrast, for the regime $\omega \ll \Gamma$ relevant for STM experiments,² the ionic state survives for much less

²Typical molecular vibrational frequencies are of the order of 10–100 meV, while in STM experiments the tunneling-induced width Γ is about 0.5–1.0 eV. It is therefore reasonable to assume that $\Gamma/\omega \gg 1$ for such experiments.

than a full vibration period. Thus, the molecule returns to its original conformation with high probability, and conformational switching occurs rarely. Such low-quantum-yield switching has been observed in recent experiments [16, 27, 28]. For instance, STM measurements on azobenzene derivatives show that only one out of 10^{10} tunneling electrons induces a switching event [16].

It is this regime of low-quantum-yield switching in asymmetric molecular junctions which is the principal focus of the present paper. We focus on the regime of sequential tunneling relevant to STM experiments on passivated surfaces [29]. We present a fully analytical treatment of the quantum yield within a generic model system. Specifically, we show that the temperature dependence reflects a sensitive interplay of vibrational frequency, tunneling rates, and charge-induced vibrational deformation. Our results are obtained from a Fokker–Planck equation which incorporates the molecule–tip and molecule–substrate tunneling as well as dissipation of the vibrational degree of freedom. A crucial assumption in our approach is the quasi-classical treatment of the vibrations. In this respect, our approach is related to the formalism used for the description of transport through nanoelectromechanical systems (NEMS) that have recently received much attention [30–32].

The paper is organized as follows. In Sect. 2, we outline the model. In Sect. 3, we derive a set of quasi-classical Boltzmann equations which describes the tunneling dynamics in the absence of dissipation. In Sect. 4, the Boltzmann equation is extended to account for dissipation, resulting in a set of Fokker–Planck equations. A formal solution for the quantum yield, which is based on this Fokker–Planck equation, is derived in Sect. 5. Finally, the formal solution is analyzed in detail, both analytically and numerically, in Sect. 6. We conclude and summarize in Sect. 7. Some details are relegated to an Appendix.

2 Model

We consider a vibrating single molecule which is coupled to two reservoirs, which serve as source and drain electrodes. The vibrational potential surface of the neutral molecule is assumed to have the form of a double well representing the cis and the trans state, whereas the potential surface of the charged state is assumed to be harmonic.

Vibrational relaxation in the neutral state is assumed to be sufficiently fast so that tunneling events always start from one of the minima of the double well. This permits one to approximate the double well potential by two separate harmonic oscillators. The resulting three-level system with states $|\text{cis}\rangle$, $|\text{trans}\rangle$, $|1\rangle$ is described by the molecular Hamiltonian

$$H_{\text{mol}} = H_{\text{cis}}|\text{cis}\rangle\langle\text{cis}| + H_{\text{trans}}|\text{trans}\rangle\langle\text{trans}| + H_1|1\rangle\langle 1|, \quad (5)$$

where

$$H_s = \epsilon_s + \frac{p^2}{2m_s} + V_s(x) \quad (6)$$

denotes the vibrational Hamiltonian of subspace $s = \text{cis}, \text{trans}, 1$. The variables x , p , and m_s denote the normal coordinate, momentum, and reduced mass of the vibrational modes, and $V_s(x)$ denotes the corresponding potential within the harmonic approximation, $V_s(x) = m_s \omega_s^2 (x - x_s)^2 / 2$, with oscillator frequency ω_s and local minimum x_s . The parameter ϵ_s denotes the energies of the relevant electronic states.

The full system is modeled by the Hamiltonian

$$H = H_{\text{mol}} + H_{\text{leads}} + H_t, \quad (7)$$

where

$$H_{\text{leads}} = \sum_{\alpha k} \epsilon_k a_{\alpha k}^\dagger a_{\alpha k} \quad (8)$$

describes the noninteracting electrons in the two leads ($\alpha = \text{tip}, \text{sub}$), and

$$H_t = \sum_{\alpha k} t_\alpha a_{\alpha k}^\dagger (|\text{cis}\rangle\langle 1| + |\text{trans}\rangle\langle 1|) + \text{h.c.} \quad (9)$$

represents the tunneling between the molecule and the leads. We assume that t_α is nonzero for the $|\text{cis}\rangle \leftrightarrow |1\rangle$ ($|\text{trans}\rangle \leftrightarrow |1\rangle$) transitions when $x < x_1$ ($x > x_1$). Here $a_{\alpha k}^\dagger$ creates an electron with momentum k and energy ϵ_k in lead α . We omit the spin index of these operators, since we ignore spin-dependent transport phenomena in the following.

3 Boltzmann equation

The dynamics of the system is described by a set of Boltzmann equations, which we derive within a density-matrix formalism. The starting point is the von Neumann equation,

$$\frac{d\rho}{dt} = -\frac{i}{\hbar}[H, \rho], \quad (10)$$

for the time evolution of the density matrix ρ of the system, which has the formal iterative solution [33]

$$\begin{aligned} \frac{d\rho(t)}{dt} &= -\frac{i}{\hbar}[H_t(t), \rho(0)] \\ &\quad - \frac{1}{\hbar^2} \int_0^t dt' [H_t(t), [H_t(t'), \rho(t')]]. \end{aligned} \quad (11)$$

Here operators O with an explicit time argument are in the interaction picture,

$$O(t) = e^{i(H_{\text{mol}} + H_{\text{leads}})t/\hbar} O e^{-i(H_{\text{mol}} + H_{\text{leads}})t/\hbar}. \quad (12)$$

The dynamics of the molecule is described by the reduced density matrix which is obtained by tracing out the degrees of freedom of the leads,

$$\rho_{\text{mol}}(t) = \text{Tr}_{\text{leads}} \rho(t). \quad (13)$$

Solving (11) for ρ relies on two approximations [33]. The large-reservoir approximation allows us to write the density matrix as a direct product,

$$\rho(t) \simeq \rho_{\text{mol}}(t) \otimes \rho_{\text{leads}}, \quad (14)$$

of the density matrices $\rho_{\text{mol}}(t)$ and ρ_{leads} describing the degrees of freedom of the molecule and the leads. In addition, we neglect effects of the molecule on the leads, which are assumed to remain in separate thermal equilibria despite the applied bias voltage and which are described by Fermi distribution functions $f_{\alpha}(\epsilon) = 1/[e^{(\epsilon - \mu_{\alpha})/k_{\text{B}}T} + 1]$ at chemical potentials μ_{α} . The Markov approximation permits us to replace

$$\rho_{\text{mol}}(t') \simeq \rho_{\text{mol}}(t) \quad (15)$$

in (11) and to replace the lower limit of integration by minus infinity, which means that memory effects of the molecular dynamics are ignored.

Furthermore, we assume $\rho_{\text{mol}}(t)$ to be diagonal in the conformational degree of freedom,

$$\rho_{\text{mol}} = |\text{cis}\rangle \rho_{\text{cis}} \langle \text{cis}| + |\text{trans}\rangle \rho_{\text{trans}} \langle \text{trans}| + |1\rangle \rho_1 \langle 1|. \quad (16)$$

Superpositions of different charge states can be neglected due to superselection rules [34, 35], while superpositions of the cis and the trans state are assumed to decay rapidly due to fast vibrational relaxation in the neutral state.

Using (14)–(16), tracing out the degrees of freedom of the leads, and opening the double commutator in (11) gives

$$\begin{aligned} & \frac{d\rho_{\text{mol}}}{dt} \\ &= -\frac{i}{\hbar} [H_{\text{mol}}, \rho_{\text{mol}}] - \sum_{\alpha k} \frac{|t_{\alpha}|^2}{\hbar^2} \sum_{s=\text{cis,trans}} \int_0^{\infty} d\tau \\ & \quad \times (|s\rangle \langle s| - |1\rangle \langle 1|) \left\{ e^{i\epsilon_k \tau/\hbar} (f_{\alpha}(\epsilon_k) e^{-iH_1 \tau/\hbar} e^{iH_s \tau/\hbar} \rho_s \right. \\ & \quad \left. - [1 - f_{\alpha}(\epsilon_k)] \rho_1 e^{-iH_1 \tau/\hbar} e^{iH_s \tau/\hbar} \right\} + \text{h.c.} \end{aligned} \quad (17)$$

Going to the Wigner representation of the density matrix,

$$W_s(x, p) = \int \frac{dy}{2\pi\hbar} e^{-ipy/\hbar} \left\langle x + \frac{y}{2} \left| \rho_s \right| x - \frac{y}{2} \right\rangle, \quad (18)$$

allows for a semiclassical description of the vibrational modes, where, in the quasiclassical limit, the Wigner function $W_s(x, p)$ describes the probability of finding the oscillator in state $s = \text{cis, trans, 1}$ at position x with momentum p .

The Wigner transform of the terms in (17) is evaluated for the slow-resonator limit, $\omega_s \ll \Gamma$, and the sequential tunneling limit, $k_{\text{B}}T \gg \hbar\Gamma$. Details on the calculation are explained in the Appendix. One finally arrives at the following set of Boltzmann equations,

$$\frac{\partial W_s}{\partial t} = \{\mathcal{H}_s, W_s\} + R_{1 \rightarrow s} W_1 - R_{s \rightarrow 1} W_s, \quad (19a)$$

$$\frac{\partial W_1}{\partial t} = \{\mathcal{H}_1, W_1\} + \sum_s (R_{s \rightarrow 1} W_s - R_{1 \rightarrow s} W_1), \quad (19b)$$

for $s = \text{cis, trans}$, with transition rates which are equivalent to Fermi's Golden Rule,

$$R_{s \rightarrow 1}(x, p) = \sum_{\alpha} \Gamma_{\alpha} f_{\alpha}(\mathcal{H}_1(x, p) - \mathcal{H}_s(x, p)), \quad (20a)$$

$$R_{1 \rightarrow s}(x, p) = \sum_{\alpha} \Gamma_{\alpha} [1 - f_{\alpha}(\mathcal{H}_1(x, p) - \mathcal{H}_s(x, p))]. \quad (20b)$$

Here $\mathcal{H}_s(x, p) = \epsilon_s + p^2/2m_s + V_s(x)$ is the Wigner transform of the harmonic-oscillator Hamiltonian, and $\Gamma_{\alpha} = 2\pi |t_{\alpha}|^2 \nu_{\alpha}/\hbar$, where ν_{α} denotes the density of states in lead α , which we take as a constant. The Poisson bracket appearing in (19) is defined as

$$\{\mathcal{H}_s, W_s\} = \frac{\partial \mathcal{H}_s}{\partial x} \frac{\partial W_s}{\partial p} - \frac{\partial \mathcal{H}_s}{\partial p} \frac{\partial W_s}{\partial x}. \quad (21)$$

Note that all rates in (20) depend only on x and not on p if one assumes equal reduced masses m_s for all vibrational modes.

4 Fokker–Planck equation

The set of Boltzmann equations derived in the previous section does not have a unique stationary solution in the absence of electronic tunneling. In this case, (19) is solved by any function W_s that depends on \mathcal{H}_s only, since the Poisson brackets then vanish exactly. However, a unique solution is obtained if we add the coupling to a bath, which takes into account the damping of the vibrations such that the system is driven back towards (local) equilibrium. The relaxation of the molecular vibron due to the presence of a bosonic bath can be modeled by the Caldeira–Leggett Hamiltonian [36–38],

$$H_{\text{CL}} = H_{\text{vib}} + H_{\text{bath}} + H_{\text{coupling}}, \quad (22)$$

where

$$H_{\text{vib}} = \hbar\omega b^{\dagger} b \quad (23)$$

describes the vibron,

$$H_{\text{bath}} = \sum_q \hbar \omega_q b_q^\dagger b_q \tag{24}$$

a bath of harmonic oscillators, and

$$H_{\text{coupling}} = \hbar g (b^\dagger + b) \sum_q (b_q^\dagger + b_q) \tag{25}$$

the linear coupling between them. Here b_q^\dagger creates a phonon in the reservoir with frequency ω_q , and g determines the coupling strength. Treating both the bosonic and fermionic coupling to the leads perturbatively, we obtain a set of Fokker–Planck equations [36–38],

$$\begin{aligned} \frac{\partial W_s}{\partial t} = & \{ \mathcal{H}_s, W_s \} + R_{1 \rightarrow s} W_1 - R_{s \rightarrow 1} W_s + \gamma_s \frac{\partial}{\partial p} p W_s \\ & + \frac{\gamma_s}{2} m_s \hbar \omega_s \coth \left(\frac{\hbar \omega_s}{2 k_B T} \right) \frac{\partial^2}{\partial p^2} W_s, \end{aligned} \tag{26a}$$

$$\begin{aligned} \frac{\partial W_1}{\partial t} = & \{ \mathcal{H}_1, W_1 \} + \sum_s (R_{s \rightarrow 1} W_s - R_{1 \rightarrow s} W_1) + \gamma_1 \frac{\partial}{\partial p} p W_1 \\ & + \frac{\gamma_1}{2} m_1 \hbar \omega_1 \coth \left(\frac{\hbar \omega_1}{2 k_B T} \right) \frac{\partial^2}{\partial p^2} W_1, \end{aligned} \tag{26b}$$

to lowest nonvanishing order in $\hbar g$. The damping rate $\gamma_s = 2\pi g^2 \sum_q \delta(\omega_s - \omega_q)$ determines the magnitude of the drift (terms proportional to the first derivative with respect to the momentum) and diffusive motion (terms proportional to the second derivative). Note that our calculation ignores any effects of dissipation on the tunneling rates.

In the absence of electronic tunneling, the stationary solutions of (26) reduce to Gaussian distribution functions,

$$W_s \sim \exp \left[- \frac{\mathcal{H}_s(x, p)}{\hbar \omega_s \coth(\hbar \omega_s / 2 k_B T) / 2} \right], \tag{27}$$

where $s = \text{cis, trans, } 1$. If the vibrational energy is larger than the thermal energy, $\hbar \omega_s \gg k_B T$, one obtains the occupation probabilities of the ground state wave function of the harmonic oscillator, whereas for the reverse case, $\hbar \omega_s \ll k_B T$, one obtains Boltzmann distribution functions.

5 Quantum yield

The Fokker–Planck equation derived in Sect. 4 allows us to investigate the current-induced conformational switching dynamics of the molecule. Specifically, we are interested in the *quantum yield* which is the probability for a single electron tunneling through the system to switch the molecule. We calculate this quantity as the conditional probability for the molecule to go, say, into the trans state in the first tunneling event after excitation from the cis state into the charged state at time $t = 0$.

We are interested in the regime where the molecule spends almost all the time in the neutral state, i.e., either in the cis or in the trans conformation, due to very asymmetric couplings to the leads. The rate for electronic tunneling from the molecule into the leads is assumed to be much higher than all vibrational frequencies, $\omega_s \ll \Gamma$. Shortly after a transition from the cis state to the charged state, the two Wigner functions W_{cis} and W_{trans} are equal to zero. In this case, the equations of motion (26) simplify to

$$\begin{aligned} \frac{\partial W_{\text{cis}}}{\partial t} = & \{ \mathcal{H}_{\text{cis}}, W_{\text{cis}} \} + R_{1 \rightarrow \text{cis}} W_1 + \gamma_{\text{cis}} \frac{\partial}{\partial p} p W_{\text{cis}} \\ & + \frac{\gamma_{\text{cis}}}{2} m_{\text{cis}} \hbar \omega_{\text{cis}} \coth \left(\frac{\hbar \omega_{\text{cis}}}{2 k_B T} \right) \frac{\partial^2}{\partial p^2} W_{\text{cis}}, \end{aligned} \tag{28}$$

$$\begin{aligned} \frac{\partial W_{\text{trans}}}{\partial t} = & \{ \mathcal{H}_{\text{trans}}, W_{\text{trans}} \} + R_{1 \rightarrow \text{trans}} W_1 \\ & + \gamma_{\text{trans}} \frac{\partial}{\partial p} p W_{\text{trans}} \\ & + \frac{\gamma_{\text{trans}}}{2} m_{\text{trans}} \hbar \omega_{\text{trans}} \coth \left(\frac{\hbar \omega_{\text{trans}}}{2 k_B T} \right) \frac{\partial^2}{\partial p^2} W_{\text{trans}}, \end{aligned} \tag{29}$$

$$\frac{\partial W_1}{\partial t} = \{ \mathcal{H}_1, W_1 \} - (R_{1 \rightarrow \text{cis}} + R_{1 \rightarrow \text{trans}}) W_1. \tag{30}$$

We need not include any rates out of the cis and trans states, since we are only interested in the first out-scattering event. The drift and diffusion terms in (30) for the charged state have been neglected. This is justified since the switching dynamics is controlled by times $t \sim 1/\omega_s$ beyond which $W_1(t)$ is exponentially suppressed. In contrast, dissipation becomes relevant for much later times of order $1/\gamma_s$. Note also that the dissipative terms in the other two equations do not change the overall probability to be in one of the charge states, but only the detailed form of the distribution function within each charge states. Consequently, dissipation affects the quantum yield only through the initial vibrational distribution function after an electron tunnels from the tip to the molecule.

It is convenient to introduce action and angle variables (S and θ) for the charged state,

$$x = - \sqrt{\frac{2S}{m_1 \omega_1}} \cos \theta, \quad p = \sqrt{2m_1 \omega_1 S} \sin \theta, \tag{31}$$

since this transformation generates a cyclic variable and reduces the Poisson bracket to the simple form

$$\{ \mathcal{H}_1, W_1 \} = -\omega_1 \frac{\partial W_1}{\partial \theta}. \tag{32}$$

Since (30) does not contain W_{cis} and W_{trans} , it can thus be solved independently,

$$W_1(\theta, S, t) = W_1(\theta - \omega_1 t, S, t = 0)$$

$$\times \exp \left[- \int_0^t dt' \sum_s R_{1 \rightarrow s}(\theta - \omega_1 t', S) \right]. \quad (33)$$

We can now insert this result into (29). Integrating over phase space yields

$$\begin{aligned} & \int d\theta dS W_{\text{trans}}(\theta, S, t) \\ &= \int d\theta dS R_{1 \rightarrow \text{trans}}(\theta, S) \\ & \quad \times \int_0^t dt' W_1(\theta - \omega_1 t', S, t=0) \\ & \quad \times \exp \left[- \int_0^{t'} dt'' \sum_s R_{1 \rightarrow s}(\theta - \omega_1 t'', S) \right], \end{aligned} \quad (34)$$

where we made use of the fact that the integral of the Poisson bracket over phase space vanishes.

The quantum yield is the total probability of going into any trans state with position x and momentum p at any time $t > 0$,

$$Y = \lim_{t \rightarrow \infty} \int d\theta dS W_{\text{trans}}(\theta, S, t). \quad (35)$$

First we calculate the *partial quantum yield*, $y(\theta_0, S_0)$, which is obtained if one assumes a delta function in phase space for the initial distribution function of the charged molecule, $W_1(\theta, S, t=0) = \delta(S - S_0) \delta(\theta - \theta_0)$. Then the total quantum yield Y can be computed as an average over all possible initial conditions $W_1(\theta, S, t=0)$,

$$Y = \int d\theta dS W_1(\theta, S, t=0) y(\theta, S). \quad (36)$$

For the partial quantum yield, we obtain

$$\begin{aligned} y(\theta, S) &= \int_0^\infty dt' R_{1 \rightarrow \text{trans}}(\theta + \omega_1 t', S) \\ & \quad \times \exp \left[- \int_0^{t'} dt'' \sum_s R_{1 \rightarrow s}(\theta + \omega_1 t'', S) \right]. \end{aligned} \quad (37)$$

Note that it depends on both x_{cis} and x_{trans} because of the position dependence of the rates $R_{1 \rightarrow \text{cis}}$ and $R_{1 \rightarrow \text{trans}}$. Making use of the periodicity of the rates in θ , we can perform the integrations over complete periods, $T_1 = 2\pi/\omega_1$, and obtain

$$\begin{aligned} y(\theta, S) &= \int_0^{T_1} dt' R_{1 \rightarrow \text{trans}}(\theta + \omega_1 t', S) \\ & \quad \times \frac{\exp \left[- \int_0^{t'} dt'' \sum_s R_{1 \rightarrow s}(\theta + \omega_1 t'', S) \right]}{1 - \exp \left[- \int_0^{T_1} dt'' \sum_s R_{1 \rightarrow s}(\theta + \omega_1 t'', S) \right]}. \end{aligned} \quad (38)$$

In the regime of our interest, where the tunneling rate is large compared to the oscillation frequency, $\omega_1 \ll \Gamma$, the exponential in the denominator is very close to zero and can be neglected, so that

$$\begin{aligned} y(\theta, S) &\simeq \int_0^{T_1} dt' R_{1 \rightarrow \text{trans}}(\theta + \omega_1 t', S) \\ & \quad \times \exp \left[- \int_0^{t'} dt'' \sum_s R_{1 \rightarrow s}(\theta + \omega_1 t'', S) \right]. \end{aligned} \quad (39)$$

This result has a clear physical interpretation. The exponential describes the conditional probability that the molecule starting at phase space point S and θ at time $t'' = 0$ is still in the charged state at time $t'' = t'$.

6 Results and discussion

In what follows, we assume for simplicity that the three oscillators of the cis, trans, and charged states centered at x_{cis} , x_{trans} , and $x_1 = 0$, respectively, all have the same reduced mass m and frequency ω . The damping rate is thus the same for all vibrational states, and we denote it as γ .

The regime of interest is characterized by the inequalities

$$\Gamma_{\text{tip}} \ll \omega \ll \Gamma_{\text{sub}}. \quad (40)$$

Moreover, we will assume that the tip-to-molecule tunneling is sufficiently weak,

$$\Gamma_{\text{tip}} \ll \gamma \ll \omega, \quad (41)$$

so that the vibrational mode thermally equilibrates in both the cis and trans conformation after each tunneling event. The nonequilibrium regime $\Gamma_{\text{tip}} \gg \gamma$ is clearly interesting but beyond the scope of the present paper.

It is natural to assume that the asymmetric molecule-electrode coupling goes along with asymmetric voltage drops (although the latter are determined by capacitive couplings rather than tunnel amplitudes). To be specific, we will assume that the voltage $V = V_{\text{tip}} - V_{\text{sub}}$ drops entirely between tip and molecule,

$$V_{\text{tip}} \simeq V, \quad V_{\text{sub}} \simeq 0. \quad (42)$$

This has important consequences for the electronic transport. Energy conservation for the electronic tunneling from the cis state into the charged state requires

$$\epsilon_1 - \epsilon_{\text{cis}} + V_1(x) - V_{\text{cis}}(x) < V_{\text{tip}}. \quad (43)$$

In the vicinity of $x \simeq x_{\text{cis}}$, this condition reduces to

$$\epsilon_1 - \epsilon_{\text{cis}} + \frac{1}{2} m \omega^2 x_{\text{cis}}^2 < V_{\text{tip}}, \quad (44)$$

which defines a threshold voltage beyond which tunneling from tip to molecule becomes possible. For voltages not too far below this threshold, tunneling from the molecule into the substrate is always energetically possible, since the corresponding condition for energy conservation,

$$\epsilon_1 - \epsilon_{\text{cis}} + V_1(x) - V_{\text{cis}}(x) > V_{\text{sub}}, \tag{45}$$

is always satisfied for sufficiently large values of $\epsilon_1 - \epsilon_{\text{cis}}$ and $V_{\text{sub}} \simeq 0$.

When the bias exceeds the threshold value $V_c = \epsilon_1 - \epsilon_{\text{cis}} + m\omega^2 x_{\text{cis}}^2/2$, the steady-state current through the molecule is given by

$$I_{\text{cis}} \simeq e \Gamma_{\text{tip}}, \tag{46}$$

i.e., it is essentially governed by the slower tip-to-molecule tunneling. Due to the Franck–Condon principle, the vibrational distribution function in the cis state will be left unaltered during the tunneling process. Due to the assumption $\Gamma_{\text{tip}} \ll \gamma$ and for thermal energies $k_B T \gg \hbar\omega$, the stationary solution of (26) in absence of tunneling reduces to a Boltzmann distribution function, cf. (27). Thus the initial distribution function of the charged state is

$$W_1(\theta, S, t = 0) = \frac{\omega}{2\pi k_B T} \exp\left[-\frac{\mathcal{H}_{\text{cis}}(\theta, S) - \epsilon_{\text{cis}}}{k_B T}\right]. \tag{47}$$

Notice that if the bias voltage is in the vicinity of the threshold voltage V_c , the distribution function becomes truncated during tunneling due to energetic restrictions. Apart from the initial distribution function, the switching dynamics is mostly determined by tunneling processes from the molecule into the substrate. Since these processes are not affected by energetic restrictions, their rates are essentially constant, independent of temperature and bias.

We begin our analytical analysis by deriving the partial quantum yield $y(\theta, S)$. We approximate $R_{1 \rightarrow \text{trans}}(\theta, S) = \Gamma_{\text{sub}}$ for $|\theta| > \pi/2$ and zero otherwise. Similarly, we take $R_{1 \rightarrow \text{cis}}(\theta, S) = \Gamma_{\text{sub}}$ for $|\theta| < \pi/2$. Then, we find for $\omega \ll \Gamma_{\text{sub}}$

$$y(\theta) \simeq \exp\left[-\frac{\Gamma_{\text{sub}}}{\omega} \left(\frac{\pi}{2} - \theta\right)\right]. \tag{48}$$

Note that the quantum yield depends only on the phase space angle θ and not on the action coordinate S . This is a direct consequence of the harmonic potential surface. Phase space angles $\theta > 0$ correspond to positive initial velocities and thus lead to a higher quantum yield as compared to $\theta < 0$. Plots of the partial quantum yield for different values of $\Gamma_{\text{sub}}/\omega$ are shown in Fig. 2.

For $\theta = 0$, the partial quantum yield is approximately $\exp(-\Gamma_{\text{sub}}\pi/2\omega)$. This result has a simple physical interpretation, since $\pi/2\omega$ is just a quarter period of the harmonic motion on the potential surface.

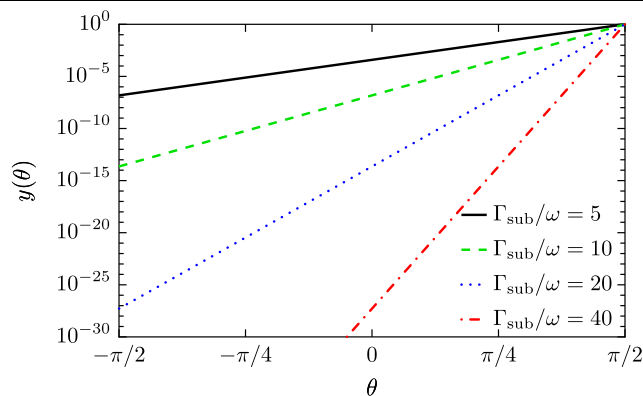


Fig. 2 Partial quantum yield $y(\theta)$ as a function of phase space angle θ for different frequency ratios of the electronic tunneling rate Γ_{sub} and the vibrational frequency ω

For the case where the initial distribution function $W_1(\theta, S, t = 0)$ is given by (47), i.e., the thermal distribution in the cis state, the total quantum yield is readily obtained from (36) and (39),

$$Y = \frac{\omega}{2\pi k_B T} \exp\left(-\frac{m\omega^2 x_{\text{cis}}^2}{2k_B T}\right) \times \int_{-\pi/2}^{+\pi/2} d\theta \exp\left[-\frac{\Gamma_{\text{sub}}}{\omega} \left(\frac{\pi}{2} - \theta\right)\right] \times \int_0^\infty dS \exp\left(-\frac{\omega S}{k_B T} + \frac{m\omega^2 |x_{\text{cis}}|}{k_B T} \sqrt{\frac{2S}{m\omega}} \cos\theta\right). \tag{49}$$

We now change the action variable to $J = \omega S/k_B T$ and introduce the large parameter $L = m\omega^2 x_{\text{cis}}^2/2k_B T$. Moreover, it is useful to write the second large parameter $\Gamma_{\text{sub}}/\omega = \alpha L$, where α denotes the ratio of the two large parameters. Note that α increases with temperature and can be interpreted as a measure of temperature. With these definitions, we find

$$Y = \frac{\exp(-L)}{2\pi} \int_{-\pi/2}^{+\pi/2} d\theta \exp\left[-\alpha L \left(\frac{\pi}{2} - \theta\right)\right] \times \int_0^\infty dJ \exp(-J + 2\sqrt{LJ} \cos\theta). \tag{50}$$

If the dominant contribution to the θ -integral comes from a region which does not include $\theta \simeq \pi/2$, the integration over J can be performed by saddle-point integration due to $L \gg 1$. This can be made explicit by introducing $x = J/L$. Doing so and performing the saddle-point integration over x , we obtain

$$Y = \sqrt{\frac{L}{\pi}} \int_{-\pi/2}^{+\pi/2} d\theta \cos\theta \times \exp\left\{-L \left[\alpha \left(\frac{\pi}{2} - \theta\right) + \sin^2\theta\right]\right\}. \tag{51}$$

Finally, at sufficiently low temperatures, $\alpha < 1$, we can also perform the angular integration by the saddle-point method. Finding the saddle point, we obtain that the optimal θ is given by

$$\theta_0 = \frac{1}{2} \arcsin \alpha. \tag{52}$$

The existence of an optimal θ reflects the competition between the following trends: The larger the initial θ , the smaller is its weight in the initial distribution function, but the larger is the corresponding partial yield. Performing the saddle-point integration, we obtain our central analytical result for the quantum yield,

$$Y \simeq \left(\frac{1 + \sqrt{1 - \alpha^2}}{2\sqrt{1 - \alpha^2}} \right)^{1/2} \times \exp \left\{ -\frac{L}{2} [\alpha(\pi - \arcsin \alpha) + 1 - \sqrt{1 - \alpha^2}] \right\}. \tag{53}$$

It is instructive to analyze various limits of this equation. At very low temperatures, $\alpha \ll 1$, the expression (53) for the quantum yield takes the form

$$Y \simeq \exp \left(-\frac{\pi \Gamma_{\text{sub}}}{2 \omega} \right). \tag{54}$$

This reflects the fact that at low temperatures, the initial distribution function is very narrow and is well approximated by $\delta(S - m\omega x_{\text{cis}}^2/2)\delta(\theta)$. Thus, switching requires that the system stays for a quarter oscillation period in the charged state. At larger temperatures where α is close to but still smaller than one, we find

$$Y \simeq \frac{1}{\sqrt{2}(1 - \alpha^2)^{1/4}} \exp \left[-L \left(\frac{\pi}{4} + \frac{1}{2} \right) \right]. \tag{55}$$

This result is remarkable in that the exponential suppression is stronger than what one would expect for thermal activation, namely $\exp(-L)$. This suggests that there exists a ‘‘critical’’ temperature where there is a *sharp crossover* between current-induced switching and processes closely related to thermal activation, originating from $\theta \simeq \pi/2$.

Indeed, it is straightforward to compute the contribution to the quantum yield Y in (50) from angle variables θ in the vicinity of $\pi/2$ which were previously neglected. To do so, we start with (50), expand the exponent for $\theta \simeq \pi/2$, and obtain

$$Y_{\pi/2} \simeq \frac{L}{2\pi} \exp(-L) \times \int_0^\infty d\tilde{\theta} \int_0^\infty dJ \exp[-L(\alpha\tilde{\theta} + J - 2\sqrt{J\tilde{\theta}})]. \tag{56}$$

Changing integration variables to $t = L\tilde{\theta}$ and $j = LJ$, we note that the last term in the exponent can be neglected in the

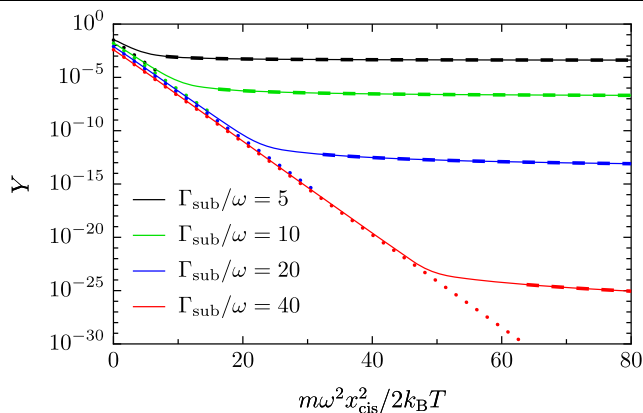


Fig. 3 Total quantum yield Y as a function of the inverse temperature $1/T$ for different ratios of the electronic tunneling rate Γ_{sub} and the vibrational frequency ω . *Solid lines*: numerical integration of (49). *Dashed lines*: quantum yield for $T < T_c$ (53). *Dotted lines*: quantum yield for $T > T_c$ (57)

limit of large L . Then, the integration becomes elementary, and we obtain

$$Y_{\pi/2} \simeq \frac{\omega}{2\pi \Gamma_{\text{sub}}} \exp(-L). \tag{57}$$

Thus, we indeed confirm that for α close to unity, the dominant contribution is no longer current-induced switching, but rather thermal-activation processes. Since $L \gg 1$, there is a sharp crossover between both behaviors when the exponents in (53) and (57) coincide. This happens for a critical α_c determined by

$$\frac{\alpha_c}{2} (\pi - \arcsin \alpha_c) = \sqrt{1 - \alpha_c^2}, \tag{58}$$

which yields $\alpha_c \simeq 0.63$.

The critical α_c translates into a critical temperature

$$k_B T_c = \alpha_c \frac{\omega}{\Gamma_{\text{sub}}} \frac{m\omega^2 x_{\text{cis}}^2}{2}. \tag{59}$$

For $T < T_c$, cis-trans switching is dominated by current-induced switching, while thermal activation takes over for $T > T_c$. Since L is typically a large parameter, this crossover will typically be sharp. It is important to note that this crossover occurs long before the thermal broadening of the initial distribution function becomes comparable to $|x_{\text{cis}}|$.

These analytical results are compared to numerical evaluations of (49) in Fig. 3 (solid lines), where the quantum yield is shown as a function of temperature. For $T < T_c$, the yield can be approximated by the expression for current-induced switching (dashed lines, (53)), while for $T > T_c$, it is mostly thermally activated (dotted lines, (57)). The existence of a sharp transition for T close to T_c can be clearly seen in the figure.

7 Summary and conclusions

In this paper, we have analyzed the current-induced conformational switching in single-molecule junctions. Our study is motivated by recent STM experiments on azobenzene derivatives, which we model as having two stable conformations in the neutral state (cis and trans), while the potential surface of the charged molecule only exhibits a single minimum (Fig. 1(e)). Current flow through such a conformational switch is characterized by telegraph noise since the two conformations will in general be characterized by different conductances and switching between the conformations occurs rarely.

As appropriate for STM setups, we consider a molecular junction with strongly asymmetric coupling to tip and substrate and treat current flow within the sequential tunneling approximation. The latter is justified in setups with passivated substrates. Our central finding is that there exists a rather sharp crossover between two qualitatively different switching mechanisms as a function of temperature. For low temperatures, the switching process is induced by tunneling electrons when the vibrational coordinate is close to the minimum of the cis state. We call this process current-induced switching. Beyond a critical temperature, switching is strongly dominated by tunneling processes which occur close to the maximum of the barrier between the cis and the trans states. We refer to this process as thermally activated. Remarkably, this happens long before the temperature becomes of the order of the barrier height.

Experimentally, the two switching mechanisms are readily distinguished by their different temperature dependences. While the current-induced switching exhibits only weak temperature sensitivity, thermal activation processes follow Arrhenius behavior, see Fig. 3. Moreover, our results predict that the quantum yield depends exponentially on the tunneling rate to the substrate which makes it highly sensitive to the level of passivation of the substrate.

Our results leave several avenues for future research. It would be interesting to analyze the quantum yield as a function of voltage for voltages in the vicinity of the threshold for tip-to-molecule tunneling. Most important would be an extension to include the resonant broadening of the molecular orbital by the molecule-substrate coupling, which would make our results applicable to experiments with non-passivated substrates.

Acknowledgements We would like to thank J.I. Pascual for helpful discussions. Support by the Deutsche Forschungsgemeinschaft through Sfb 658 as well as the BMBF through DIP is gratefully acknowledged.

Appendix

In this Appendix, we show how to obtain the Boltzmann equation (19) from the master equation (17) in the sequen-

tial tunneling regime. We assume that the oscillators of the cis, trans, and charged states centered at x_{cis} , x_{trans} , and $x_1 = 0$, respectively, all have the same reduced mass m and frequency ω , which allows all calculations to be done explicitly. It is evident that the underlying arguments also extend to the more general case.

Projecting (17) on, say, the cis state (the derivation for the two other states proceeds analogously), we obtain

$$\begin{aligned} \frac{d\rho_{\text{cis}}}{dt} = & -\frac{i}{\hbar}[H_{\text{cis}}, \rho_{\text{cis}}] - \sum_{\alpha k} \frac{|t_{\alpha}|^2}{\hbar^2} \int_0^{\infty} d\tau \\ & \times \left\{ e^{i\epsilon_k \tau/\hbar} (f_{\alpha}(\epsilon_k) e^{-iH_1 \tau/\hbar} e^{iH_{\text{cis}} \tau/\hbar} \rho_{\text{cis}} \right. \\ & \left. - [1 - f_{\alpha}(\epsilon_k)] \rho_1 e^{-iH_1 \tau/\hbar} e^{iH_{\text{cis}} \tau/\hbar} \right\} + \text{h.c.} \end{aligned} \quad (60)$$

The Wigner transform of this equation reads

$$\begin{aligned} \frac{\partial}{\partial t} W_{\text{cis}}(x, p) = & \{ \mathcal{H}_{\text{cis}}(x, p), W_{\text{cis}}(x, p) \} - 2 \sum_{\alpha k} \frac{|t_{\alpha}|^2}{\hbar^2} \\ & \times \text{Re} \int_0^{\infty} d\tau e^{\frac{i}{\hbar}[(\epsilon_k + \epsilon_{\text{cis}} - \epsilon_1)\tau - p\tilde{x}_{\tau} - (x - \frac{x_{\text{cis}}}{2})\tilde{p}_{\tau}]} \\ & \times \left\{ f_{\alpha}(\epsilon_k) W_{\text{cis}}\left(x - \frac{\tilde{x}_{\tau}}{2}, p + \frac{\tilde{p}_{\tau}}{2}\right) \right. \\ & \left. - [1 - f_{\alpha}(\epsilon_k)] W_1\left(x + \frac{\tilde{x}_{\tau}}{2}, p - \frac{\tilde{p}_{\tau}}{2}\right) \right\} \end{aligned} \quad (61)$$

with $\tilde{x}_{\tau} = x_{\text{cis}}[\cos(\omega\tau) - 1]$ and $\tilde{p}_{\tau} = m\omega x_{\text{cis}} \sin(\omega\tau)$. The first term in the right-hand side in (61) denotes the Poisson bracket between the classical Hamiltonian and the Wigner function of the cis state.

Computing the sum over momenta k in the wide-band limit, one realizes that the integrand in (61) decays exponentially with the temperature. Since we are considering the slow-vibration limit ($\omega \ll \Gamma$) and the sequential-tunneling regime ($\hbar\Gamma \ll k_B T$), we can therefore expand (61) for $\omega\tau \ll 1$ to obtain

$$\begin{aligned} \frac{\partial}{\partial t} W_{\text{cis}}(x, p) \simeq & \{ \mathcal{H}_{\text{cis}}(x, p), W_{\text{cis}}(x, p) \} \\ & - 2 \sum_{\alpha k} \frac{|t_{\alpha}|^2}{\hbar^2} \text{Re} \int_0^{\infty} d\tau e^{\frac{i}{\hbar}[\epsilon_k + \epsilon_{\text{cis}} - \epsilon_1 - m\omega^2 x_{\text{cis}}(x - x_{\text{cis}}/2)\tau]} \\ & \times \{ f_{\alpha}(\epsilon_k) W_{\text{cis}}(x, p) - [1 - f_{\alpha}(\epsilon_k)] W_1(x, p) \}. \end{aligned} \quad (62)$$

The remaining integral over τ is easily evaluated and guarantees energy conservation for the rates entering the Boltzmann equation (19).

References

1. H. Park, J. Park, A.K.L. Lim, E.H. Anderson, A.P. Alivisatos, P.L. McEuen, *Nature* **407**, 57 (2000)
2. R.H.M. Smit, Y. Noat, C. Untiedt, N.D. Lang, M.C. van Hemert, J.M. van Ruitenbeek, *Nature* **419**, 906 (2002)
3. J. Park, A.N. Pasupathy, J.I. Goldsmith, C. Chang, Y. Yaish, J.R. Petta, M. Rinkoski, J.P. Sethna, H.D. Abruna, P.L. McEuen, D.C. Ralph, *Nature* **417**, 722 (2002)
4. H.B. Heersche, Z. de Groot, J.A. Folk, H.S.J. van der Zant, C. Romeike, M.R. Wegewijs, L. Zobbi, D. Barreca, E. Tondello, A. Cornia, *Phys. Rev. Lett.* **96**, 206801 (2006)
5. M.H. Jo, J.E. Grose, K. Baheti, M. Deshmukh, J.J. Sokol, E.M. Rumberger, D.N. Hendrickson, J.R. Long, H. Park, D.C. Ralph, *Nano Lett.* **6**, 2014 (2006)
6. T. Dadoosh, Y. Gordin, R. Krahn, I. Khivrich, D. Mahalu, V. Frydman, J. Sperling, A. Yacoby, I. Bar-Joseph, *Nature* **436**, 677 (2005)
7. L.H. Yu, Z.K. Keane, J.W. Ciszek, L. Cheng, J.M. Tour, T. Baruah, M.R. Pederson, D. Natelson, *Phys. Rev. Lett.* **95**, 256803 (2005)
8. S. Braig, K. Flensberg, *Phys. Rev. B* **68**, 205324 (2003)
9. G.A. Kaat, K. Flensberg, *Phys. Rev. Lett.* **71**, 155408 (2005)
10. A. Mitra, I. Aleiner, A.J. Millis, *Phys. Rev. B* **69**, 245302 (2004)
11. J. Koch, F. von Oppen, *Phys. Rev. Lett.* **94**, 206804 (2005)
12. J. Koch, M.E. Raikh, F. von Oppen, *Phys. Rev. Lett.* **96**, 056803 (2006)
13. F. Elste, C. Timm, *Phys. Rev. B* **73**, 235305 (2006)
14. M. Galperin, M.A. Ratner, A. Nitzan, *J. Phys.: Condens. Matter* **19**, 103201 (2007)
15. A.V. Danilov, S.E. Kubatkin, S.G. Kafanov, K. Flensberg, T. Bjørnholm, *Nano Lett.* **6**, 2184 (2006)
16. N. Henningsen, K.J. Franke, I.F. Torrente, G. Schulze, B. Prieswisch, K. Rück-Braun, J. Dokic, T. Klamroth, P. Saalfrank, J.I. Pascual, *J. Phys. Chem. C* **111**, 14843 (2007)
17. A. Donarini, M. Grifoni, K. Richter, *Phys. Rev. Lett.* **97**, 166801 (2006)
18. J. Gaudio, L.J. Lauhon, W. Ho, *Phys. Rev. Lett.* **85**, 1918 (2000)
19. X.H. Qiu, G.V. Nazin, W. Ho, *Phys. Rev. Lett.* **93**, 196806 (2004)
20. M. Alemani, M.V. Peters, S. Hecht, K.H. Rieder, F. Moresco, L. Grill, *J. Am. Chem. Soc.* **128**, 14446 (2006)
21. J. Henzl, T. Bredow, K. Morgenstern, *Chem. Phys. Lett.* **435**, 278 (2007)
22. S. Gao, M. Persson, B.I. Lundqvist, *Phys. Rev. B* **55**, 4825 (1997)
23. W.H.A. Thijssen, D. Djukic, A.F. Otte, R.H. Bremmer, J.M. van Ruitenbeek, *Phys. Rev. Lett.* **97**, 226806 (2006)
24. B.-Y. Choi, S.-J. Kahng, S. Kim, H. Kim, H.W. Kim, Y.J. Song, J. Ihm, Y. Kuk, *Phys. Rev. Lett.* **96**, 156106 (2006)
25. M. del Valle, R. Gutiérrez, C. Tejedor, G. Cuniberti, *Nat. Nanotechnol.* **2**, 176 (2007)
26. G. Füchsel, T. Klamroth, J. Dokic, P. Saalfrank, *J. Phys. Chem. B* **110**, 16337 (2006)
27. V. Iancu, S.-W. Hla, *Proc. Natl. Acad. Sci.* **103**, 13718 (2006)
28. J. Henzl, M. Mehlhorn, H. Gawronski, K.H. Rieder, K. Morgenstern, *Angew. Chem. Int. Ed.* **45**, 603 (2006)
29. X.H. Qiu, G.V. Nazin, W. Ho, *Science* **299**, 542 (2003)
30. L.Y. Gorelik, A. Isacsson, M.V. Voinova, B. Kasemo, R.I. Shekhter, M. Jonson, *Phys. Rev. Lett.* **80**, 4526 (1998)
31. T. Novotny, A. Donarini, A.-P. Jauho, *Phys. Rev. Lett.* **90**, 256801 (2003)
32. T. Novotny, A. Donarini, C. Flindt, A.-P. Jauho, *Phys. Rev. Lett.* **92**, 248302 (2004)
33. K. Blum, *Density Matrix Theory and Applications*, 2nd edn. (Plenum, New York, 1996)
34. W.H. Zurek, *Phys. Rev. D* **26**, 1862 (1982)
35. D. Giulini, C. Kiefer, H.D. Zeh, *Phys. Lett. A* **199**, 291 (1995)
36. A.O. Caldeira, A.J. Leggett, *Phys. Rev. Lett.* **46**, 211 (1981)
37. A.O. Caldeira, A.J. Leggett, *Physica A* **121**, 587 (1983)
38. A.O. Caldeira, A.J. Leggett, *Physica A* **130**, 374 (1985)